DATA PAPER

LAMOST medium-resolution spectroscopic survey of binarity and exotic star (LAMOST-MRS-B): Observation strategy and target selection

Jiao Li(李蛟)[1,†], Jiang-Dan Li(李江丹)[2,3], Yan-Jun Guo(郭彦君)[2,3], Zhan-Wen Han(韩占文)[2], Xue-Fei Chen(陈雪飞)[2], Chao Liu(刘超)[1,‡], Hong-Wei Ge(葛宏伟)[2], Deng-Kai Jiang(姜登凯)[2], Li-Fang Li(李立芳)[2], Bo Zhang(章博)[1], Jia-Ming Liu(刘佳明)[5], Hao Tian(田浩)[1], Hao-Tong Zhang(张昊彤)[4], Hai-Long Yuan(袁海龙)[4], Wen-Yuan Cui(崔文元)[5], Juan-Juan Ren(任娟娟)[1], Jing-Hao Cai(蔡靖豪)[2,3], and Jian-Rong Shi(施建荣)[4]

[1] *Key Laboratory of Space Astronomy and Technology, National Astronomical Observatories, Chinese Academy of Sciences, Beijing* 100101, *China*
[2] *Yunnan Observatories, Chinese Academy of Sciences, Kunming* 650011, *China*
[3] *School of Astronomy and Space Science, University of Chinese Academy of Sciences, Beijing* 100049, *China*
[4] *Key Laboratory of Optical Astronomy, National Astronomical Observatories, Chinese Academy of Sciences, Beijing* 100101, *China*
[5] *Department of Physics, Hebei Normal University, Shijiazhuang* 050024, *China*

(Received 29 June 2022; revised manuscript received 13 September 2022; accepted manuscript online 21 September 2022)

LAMOST-MRS-B is one of the sub-surveys of LAMOST medium-resolution ($R \sim 7500$) spectroscopic survey. It aims at studying the statistical properties (e.g., binary fraction, orbital period distribution, mass ratio distribution) of binary stars and exotic stars. We intend to observe about 30000 stars (10 mag $\leq G <$ 14.5 mag) with at least 10 visits in five years. We first planned to observe 25 plates around the galactic plane in 2018. Then the plates were reduced to 12 in 2019 because of the limitation of observation. At the same time, two new plates located at the high galactic latitude were added to explore binary properties influenced by the different environments. In this survey project, we set the identified exotic and low-metallicity stars with the highest observation priorities. For the rest of the selected stars, we gave the higher priority to the relatively brighter stars in order to obtain high quality spectra as many as possible. Spectra of 49129 stars have been obtained in LAMOST-MRS-B field and released in DR8, of which 28828 and 3375 stars have been visited more than twice and ten times with SNR $\geq$ 10, respectively. Most of the sources are B-, A-, and F-type stars with $-0.6 <$ [Fe/H] < 0.4 dex. We also obtain 347 identified variable and exotic stars and about 250 stars with [Fe/H] < -1 dex. We measure radial velocities (RVs) by using 892233 spectra of the stars. The uncertainties of RV achieve about 1 km$\cdot$s^{-1}and 10 km$\cdot$s^{-1} for 95% of late- and early-type stars, respectively. The datasets presented in this paper are available at http://www.doi.org/10.57760/sciencedb.j00113.00035.

Keywords: surveys, spectroscopy, catalogs, binary

PACS: 95.80.+p, 95.75.Fg, 95.80.+p, 97.80.−d **DOI:** 10.1088/1674-1056/ac9362

1. Introduction

Binary stars are common in the galaxy. In general, more than 50% of stars are believed to be in the form of binaries or multiple systems[1] (hereafter, we abbreviate binary and multiple systems as binary unless otherwise specified). The binary fraction increases with stellar mass.[1–3] For solar-type stars with masses around 0.8–2 $M_{\odot}$, the binary fraction is not less than 50%,[4,5] while for more massive stars ($> 8\ M_{\odot}$), the binary fraction may exceed 70%.[6] Binaries with orbital periods less than a few thousand days, would experience mass transfer during their evolution.[2,7] For example, symbiotic stars are transferring mass from the giant components to the compact components; their orbital periods range from hundreds of days to a few tens of years.[8,9] Meanwhile, over 70% of all massive stars will exchange mass with a companion.[6] We identify a close binary as the binary star would experience mass transfer for clarity.

The presence of a nearby companion will alter the stellar evolution fate. It is widely known that there are exotic objects, e.g., blue stragglers, barium stars, symbiotic stars, double degenerates, hot subdwarf stars, cataclysmic variables (CVs), pulsars, x-ray binaries, gamma-ray bursts, type Ia supernovae (SNe Ia) and double stellar black holes (BHs) which are led by the interaction of binary stars.[6,7,10] However, several crucial processes are still puzzled in the binary evolution such as mass and angular momentum loss, dynamical mass transfer and common envelope evolution. Searching for exotic objects will help us to understand how the exotic objects form and what the ultimate fate of the object is.

Stellar structure and evolution are one of the cornerstones to study galaxies. There are some strange phenomena in galaxies that are hardly explained by single stellar population synthesis (SPS), for example, the far-ultraviolet (FUV) excess in

[†]Corresponding author. E-mail: lijiao@bao.ac.cn
[‡]Corresponding author. E-mail: liuchao@nao.cas.cn

© 2023 Chinese Physical Society and IOP Publishing Ltd

the spectra of elliptical galaxies,[11] while it can be well reproduced by including the radiation of hot subdwarf stars (sdOB) resulting from binary interactions.[12] The accretion of white dwarfs (WDs) in binary stars could interpret the existence of soft x-ray band extended emissions in galaxies.[13] It has a big impact on deriving ages, masses and star formation rates of galaxies by considering the binary interaction in SPS — bianry population synthesis (BPS).[7] The cosmic re-ionization photons based on SPS models are less than the required amount by a few factors, but BPS models provide a sound physical basis for cosmic re-ionization.[14,15] In BPS study, binary samples are generated based on the parameters: the star formation rate, the initial mass function of the primary, and the statistical properties of binaries such as the mass ratio distribution, the orbital period distribution and the orbital eccentricity distribution. The evolution result of the BPS model would be different when the recipes of the initial parameters are changed. The final binary properties would also vary with the evolution. Therefor, the initially parameters can be constrained by comparing the observed statistical properties of binary with BPS models.

The statistical properties of close binary vary with the stellar mass, and metallicity. Offner *et al.* (2022) summarized that the close binary fraction increases from $\sim 20\%$ to $\sim 70\%$ as the primary stars move from $\sim 0.1M_{\odot}$ to $\sim 30M_{\odot}$ by compiling the results of observational and theoretical studies of stellar multiplicity.[3] The orbital period (or separation) distributions are different between massive stars and solar-type (and the smaller mass) stars. The orbital period distribution of massive stars is likely to follow Opik's law,[2,16] while the distribution of smaller mass satisfies the lognormal distribution.[17,18] And the peaks of the lognormal distribution increase with the primary mass, the peak reaches to $\log P/(\mathrm{day}) = 5.03$ for the solar-type stars.

Assuming the distribution of mass ratio follows a power law, the power index (γ) decreases with the mass of the primary star.[2] In addition, there is an excess of twins ($q > 0.95$) for the distribution of solar-type and smaller mass stars,[1,19,20] and the excess twins fraction might arrive at 30%.[2] Nonetheless, the excess twin fraction among massive stars is only 10% within SMA $a < 0.5$ au, and the excess cannot be detected among O-type binaries beyond $a > 0.5$ au at all.[3,6]

The relation between binary fraction (f_{b}) and metallicity has been widely studied. A few works claimed that f_{b} is not correlated[21,22] or positively correlated[23–25] with metallicity. However, with the released data of Apache Point Observatory Galactic Evolution Experiment (APOGEE)[26] survey and the Large Sky Area Multi-Object fiber Spectroscopic Telescope (LAMOST) survey,[27,28] f_{b} is found to be anti-correlated with metallicity.[20,29–33] The relation looks like to change with the primary mass as well. Raghavan *et al.* (2010) found no correlation between stellar companions and metallicity for $B-V < 0.625$, but among the redder subset (the stellar mass is smaller), metal-poor stars are more likely to have companions.[17] A similar result was also found by Liu (2019), that the f_{b} is quite flat with metallicity as $\gamma < 1.2$, while the relation is anti-correlated as $\gamma > 1.2$ (the primary mass is smaller).[34] The eccentricity distribution is a function of the period. The power-law exponent of the eccentricity distribution is $\eta = -0.3 \pm 0.2$ for $p = 3$–10 days, while is $\eta = 0.6 \pm 0.3$ for $p = 10$–500 days.[2] These indicate that the distributions of binary orbital parameters are not independent.

The clear correlation between the distributions is ambiguous, due to the absence of larger enough binary samples and the different selection bias from the current observation programs. It is not clear whether these distributions are universal, since most of works were carried out based on neighborhood stars within 100 pc.

Interaction of close binary stars would generate some peculiar stars and could influence the result of BPS, so we pay more attention to the orbital parameter distributions of close binary. After the first stage 5-year survey of LAMOST low resolution spectra (LAMOST-LRS), a median resolution spectral survey was initiated (LAMOST-MRS). As a sub-survey of LAMOST-MRS, MRS-B will provide the largest homogeneous sample with multiple observations to study the stellar multiplicity, discover more various exotic binaries under different evolutionary stages, and measure their orbital parameters.

2. LAMOST-MRS

LAMOST is a 4-meter quasi-meridian reflective Schmidt telescope with 4000 fibers installed on its 5-degree-FoV focal plane. It had obtained more than 9 million stellar spectra with spectral resolution of $R \sim 1800$ at the first stage survey from 2011 to 2018. LAMOST has appended 16 spectrographs with spectra resolution of $R \sim 7500$ during 2017.[35] A pilot program of LAMOST-MRS was performed from September 2017 to June 2018 accompanied by LAMOST-LRS. LASMOT-MRS was being executed regularly from October 2018 to June 2023, and will take about 50% nights to observe objects. The spectrographs will be switched to medium resolution mode from the 7th until the 22nd of each lunar month.

Different with the wavelength coverage of LAMOST-LRS, LAMOST-MRS covers two parts of the spectra, see Fig. 1, the blue [4950, 5350] Å and the red [6300, 6800] Å arms. For late-type stars (F-, G-, and K-type), the blue arm spectra deliver the information about 20 elemental abundances, including Li, C, Na, Mg, Si, Ca, Sc, Ti, V, Cr, Mn, Fe, Co, Ni, Cu, Ba, Y, Sm, and Nd. With those information, the radial velocities (RVs) can be constrained with precision

of about 1 km · s^{-1}. While for the early-type (O-, B-, and A-type) stars, the absorption lines are weak and sparse in the blue arm.[35] So it is better to measure RV by using the spectra of the red arm with the precision of 10 km · s^{-1}. In the meantime, the red arm spectra covers Hα, [NII], and [SII] emission lines, which are crucial to the study the galactic nebulae, such as the HII regions, the supernova remnants, the planetary nebular, etc. The Hα profile is very useful in researching on the proto-planetary disk surrounding the very young stars as well.

LAMOST-MRS is separated as time-domain (TD) and non time-domain (NT) surveys. Its scientific goals mainly include stellar multiplicity, stellar pulsation, host stars of exoplanets, star formation, emission nebulae, galactic archaeology, and open clusters. According to the scientific goals, LAMOST-MRS is divided into MRS-B (TD), MRS-K (TD),[38,39] MRS-T (TD), MRS-S (TD or NT), MRS-N (NT),[40] MRS-G (NT) fields and MRS-O (NT).[35] Each field has a PI who is responsible for the target selection. For the TD survey, a plate is observed with 3–8 single 1200 s exposures in each visit (visit is that a plate is observed in one night, no matter how many exposures it takes) within the 4-hour observation window of LAMOST. About 60% visits are assigned to the TD survey. For the NT survey, a plate is continuously observed three single 1200 s exposure in each visit.

In this paper, we mainly focus on introducing the target selection and observation strategies of MRS-B, which aims at stellar multiplicity and searching for exotic stars. We have $\sim$ 30% observation time in the TD survey. A "planid" is assigned to each LAMOST-MRS plate (pointing), and the planids of MRS-B are labeled as "TDhhmmssNddmmssB01", where "hhmmssNddmmss" denotes the equatorial coordinates of the direction center star of each plate, "N" means north.

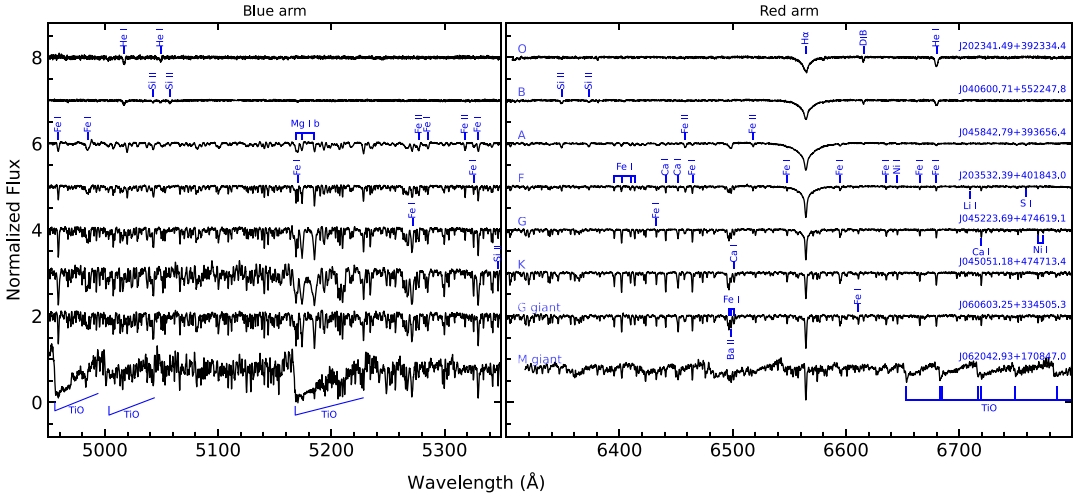


Fig. 1. The spectra example of LAMOST-MRS from late O- to M-type stars selected from LAMOST-MRS-B randomly. The spectra are normalized by following the process of Zhang *et al.* (2021).[36] Wavelengths of the spectra have been corrected to rest frame with the corresponding radial velocities. DIB is diffuse interstellar bands (6614 Å). The wavelength of TiO bands can be found in Table 6 of Valenti *et al.* (1998).[37] The wavelength of the atomic absorption lines can be found from NIST Atomic Spectra Database Lines Form.

3. Observation strategy

LAMOST-MRS is designed to observe about 4000 targets simultaneously. About 3000 stars can be observed excluding a few problematic fibers and a few hundreds of sky fibers used to obtain the skylight. There are not enough bright sources ($G < 10$ mag) to occupy all the 3000 fibers. When observing the bright sources ($G < 10$ mag), the CCD will be saturated if the same exposure time is taken as the faint source ($G \sim 14$ mag). On the other hand, if the sources are too faint, we need to take a longer exposure time to obtain spectra with a good signal-to-noise ratio (SNR), which would smear the variations of short period stars and induce more contamination from cosmic rays. Limited by the designation of LMAOST, the observation window for each target is only four hours, it means that the longer exposure time would reduce the number of exposure. Consequently, the variation of some variable stars with periods of a few hours such as RR Lyrae[41,42] will be lost. Based on the experience of LAMOST-MRS pilot program, 1200 s was used as the default exposure time to observe the sources with 10 mag $\leq G < 14.5$ mag. The SNR of the single exposure spectrum of the blue arm would be larger than 5 when $G < 14.5$ mag.

The binary stars with semi-amplitude of RV ($K > 3\sigma_{\rm rv}$) will be detected with the RV precision $\sigma_{\rm rv} \sim 1$ km · s^{-1} for late-type stars. Clearly shown in Fig. 2, LAMOST-MRS can detect the solar-type single-lined spectroscopic binaries (SB1s) with $q > 0.1$ and period $p < 1000$ days, which would experience interaction in their lifetime. We can also detect the solar-type double-lined spectroscopic binaries (SB2s) with periods $p < 50$ days because the RV difference of the two components is larger than 40 (see the top red thin horizontal lines of Fig. 2). The more massive SB2 can be detected with the longer period.

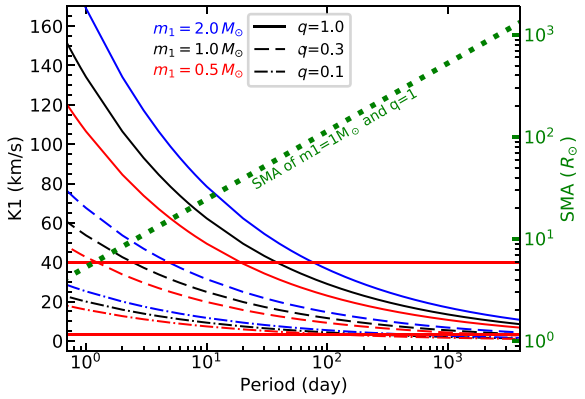


Fig. 2. The semi-amplitude of RV of primary star (semi-major aixs) as a function of period (right ordinate). Here we assume the orbital inclination and eccentricity are $i = 90°$ and $e = 0$, respectively. The blue, dark, and red lines stand for different primary masses of $m_1 = 2M_\odot$, $1M_\odot$, and $0.5M_\odot$, respectively. The solid, dashed and dash-dot lines denote the mass ratios of $q = 1$, 0.3 and 0.1, respectively. The top red thin horizontal line denotes the spectrum resolution in RV ($\delta v = c/7500 \sim 40$ km$\cdot$s^{-1}). The bottom red horizontal line with $rv = 3$ km$\cdot$s^{-1}. The green line is the SMA of binary with $m_1 = 1M_\odot$ and $q = 1$.

We would like to analyze the statistical properties by resolving binary orbital parameters (period, eccentricity, argument of pericenter, phase, and RV amplitude). According to the experiment of the Joker which is a PYTHON package of deriving orbital parameters, more than 10 observations for each star are required to obtain the reliable parameters.[43,44] In the first year (2018–2019) of LAMOST-MRS, we prepared 25 plates and took exposures as many as possible (> 3 times) when each plate passed through the observation window of LAMOST. After the observation of the first year (see Table 1), we realized that it is difficult to achieve our goal of > 10 visits for the binaries with $P > 10$ days in all 25 plates. Considering the observation strategies of MSR-K and MRS-T which have the same observational method as the first year of MRS-B (3–8 exposures each visit), the short period binaries could also be found from these two fields. Therefore, we take only three continuous 1200 s exposures in each visit in the following time.

It is hard to observe each plate with a uniform cadence (or at given dates) on account of the weather condition and the different observation strategies of the six scientific fields. It seems easier to correct the selection bias of orbital periods with random visits. So that the observation dates are randomly selected during the observation season for each plate. In order to detect binaries with period $p > 1$ year, we select two plates TD060648N233818B01 and TD203106N405128B01 to observe as long as five years.

Table 1. Plates of MRS-B field, where $N_{\rm vist}$, $N_{\rm exp}$, $N_{\rm star}$ are the number of visits (observation dates), exposure times, and observation stars, respectively. $N^{\rm 1st}_{\rm star}$ and $N^{\rm 2nd}_{\rm star}$ are the numbers of stars observed at the first and the second year of regular surveys, respectively. The plates labeled by symbols of x were not observe after October 2019 in the field of MRS-B. $*$ means that the two plates will be observed all five years of the program. TD103949N392416 and TD114941N345554 were input after October 2019. The last column stands for the number of common stars observed in both years. The observation priorities of stars were modified since the second year so that $N_{\rm star}$ is smaller than $N^{\rm 1st}_{\rm star}$ or smaller than $N^{\rm 2nd}_{\rm star}$. Note: TD043724N254338 will be observed as plate of the MRS-S field; in this table, we count all stars including the sources both $\rm SNR_B = 0$ and $\rm SNR_R = 0$.

Planid	(ra, dec)	$N_{\rm vist}$	$N_{\rm exp}$	$N^{\rm 1st}_{\rm star}$	$N_{\rm vist}$	$N_{\rm exp}$	$N^{\rm 2nd}_{\rm star}$	$N_{\rm star}$
(B01)	(°)	201810–201907			201910–202006			2018–2020
TD030224N542147	(45.60175, 54.36327)	2	7	2695	5	15	2892	2391
TD033106N502853	(52.77737, 50.48149)	2	14	2985	4	12	2909	2084
TD035400N453042	(58.50355, 45.51177)	1	6	2942	0	0	0	0
TD041114N555437	(62.81038, 55.91050)	2	11	2755	3	13	2910	2257
TD042145N500206	(65.43948, 50.03517)	3	16	3010	1	3	2807	2005
TD045606N223435	(74.02765, 22.57656)	1	8	2924	0	0	0	0
TD045704N475243	(74.26917, 47.87884)	1	8	3024	5	16	2966	2109
TD055633N285632	(89.14070, 28.94227)	2	14	3025	5	14	2956	2279
TD060648N233818*	(91.70275, 23.63860)	2	8	3076	3	9	2951	2315
TD061044N341537	(92.68602, 34.26042)	4	24	3069	2	6	2880	2163
TD062610N184524	(96.54271, 18.75690)	6	31	3213	4	11	2943	2180
TD203106N405128*	(307.77875,40.85802)	3	9	3189	0	0	0	0
TD103949N392416	(159.95557, 39.40467)	0	0	0	14	48	1884	0
TD114941N345554	(177.42381, 34.93176)	0	0	0	15	46	1713	0
TD041055N155647$^{\rm x}$	(62.72986, 15.94666)	1	4	2141	—	—	—	—
TD042649N425434$^{\rm x}$	(66.70605, 42.90949)	1	6	3000	—	—	—	—
TD043724N254338$^{\rm x}$	(69.35248, 25.72738)	2	11	2909	0	0	0	0
TD045227N391702$^{\rm x}$	(73.11599, 39.28412)	1	6	2972	—	—	—	—
TD040433N355514$^{\rm x}$	(61.14068, 35.92056)	—	—	—	—	—	—	—
TD041324N290722$^{\rm x}$	(63.35187, 29.12292)	—	—	—	—	—	—	—
TD044912N312614$^{\rm x}$	(72.30353, 31.43737)	—	—	—	—	—	—	—
TD053403N461112$^{\rm x}$	(83.51411, 46.18688)	—	—	—	—	—	—	—
TD053908N412130$^{\rm x}$	(84.78624, 41.35856)	—	—	—	—	—	—	—
TD185549N301843$^{\rm x}$	(283.95518, 30.31206)	—	—	—	—	—	—	—
TD191631N482124$^{\rm x}$	(289.12983, 48.35674)	—	—	—	—	—	—	—
TD195013N482329$^{\rm x}$	(297.55489, 48.39158)	—	—	—	—	—	—	—
TD202021N174734$^{\rm x}$	(305.08919, 17.79293)	—	—	—	—	—	—	—

4. Target selection

Most massive stars are located in the galactic disk. The companions of SB1s with early-type MS primaries may not necessarily be low-mass A–K type stars. They may contain 1–3 $M_\odot$ stellar remnants such as WDs, neutron stars, or even BHs.[45–47] In addition, the unresolved solar-type SB1s might contain compact companions as well. Most of the compact companions are WDs[48,49] accompanied by UV excess. It is useful to select solar-type + WD binary by using UV sources catalogs of the Galaxy Evolution Explorer (GALEX).[50] However, the galactic disk was not observed by the FUV-detector of GALEX (see Fig. 1 of Bianchi *et al.* 2017). To pick out these rare exotic objects as many as possible, and sufficiently utilize the 3000 fibers of LAMOST, we initially selected 25 plates around the disk (see blue + red + gray plates in Fig. 3).

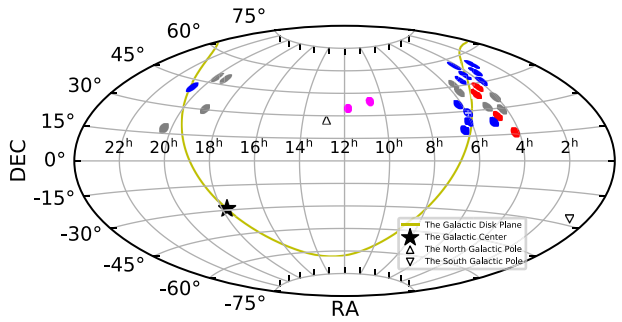


Fig. 3. The Aitoff map shows the footprints of LAMOST-MRS-B project in the celestial coordinate. The 12 blue plates will be observed in the whole 5-year LAMOST-MRS program. The four red plates were only observed at the first year (from 2018-10-05 to 2019-06-08) of the program. The two purple plates were observed from the second year (2019-10-23) of the program and the following years. The nine gray plates have been dropped out without any observation. Note: the blue field labeled white plus is TD055633N285632B01 which has the same center coordinates of HIP28117 which is a pilot program plate of LAMOST-MRS.

Numbers of massive stars (O- and B-type), sdOBs, and WDs were selected with help of *Gaia* color-magnitude diagram (CMD) as shown in Fig. 4. All those samples were set with highest observation priority in the input catalog. The massive stars were picked out with $G_{\rm BP} - G_{\rm RP} < 0$; the sdOB and WD candidates were selected by the sources under the MS stars in the CMD. Here, we did not correct the redden of $G_{\rm BP} - G_{\rm RP}$ and extinction of $M_{\rm G}$. To obtain the spectra with good qualities, for the rest of the stars with $10 \leq G < 14.5$, the observation priorities followed the rule: the stars that are in the catalog of GALEX and brighter would have higher observation priority (details see the second column of Table 2).

After the first year observation of LAMOST-MRS, we found that it is difficult to obtain > 10 visits for all the 25 plates of which only 16 plates were observed with only 34 visits. Most TD plates were crowd around the galactic disk (see Fig. 2 of Liu *et al.* 2020[35]), so they are prone to take place "traffic jams". Therefore, we droped out 13 plates (see Table 1), where TD043724N254338 would be observed in the field of MRS-S, and added two new plates located at the high galactic latitude (TD103949N392416, TD114941N345554, as shown in the purple plates of Fig. 3). We also modified the observation priorities of input catalogs on account of studying the variable stars and statistic properties of low-metallicity stars.

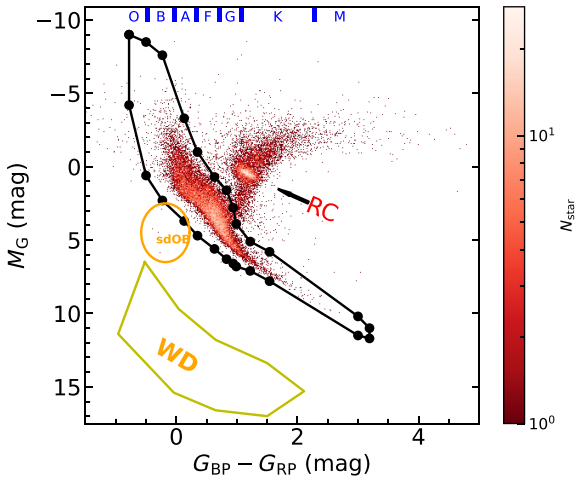


Fig. 4. *Gaia* color-magnitude diagram of source of MRS-B field in DR8. The color and G magnitude have been corrected by using *dustmaps*.[51] The black polygon indicates the location of MS stars, and its fixed points are $G_{\rm BP} - G_{\rm RP} = (-0.78, -0.5, -0.23, 0.13, 0.35, 0.63, 0.83, 0.94, 0.99, 1.22, 1.54, 3.0, 3.19, 3.19, 3.0, 1.54, 1.22, 0.99, 0.94, 0.83, 0.63, 0.35, 0.13, -0.23, -0.5, -0.78)$, $M_{\rm G} = (-9, -8.5, -7.6, -3.3, -1.0, 0.7, 1.6, 2.8, 3.9, 5.1, 5.8, 10.2, 11.0, 11.7, 11.5, 7.8, 7.1, 6.8, 6.6, 6.3, 5.6, 4.7, 3.7, 2.3, 0.6, -4.2)$. The orange curves denote the locations of sdOB and WD. RC is red clump star.

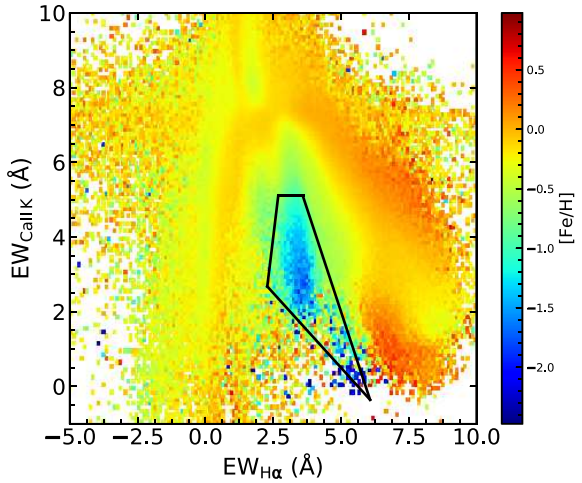


Fig. 5. Metallicity ([Fe/H]) as a function of the equivalent width of Hα and CaII K. The line indices are calculated from the spectra in the DR6 of LAMOST-LRS. The iron abundance is derived by the LAMOST pipeline. The index band-pass of Hα and CaII K is 6548–6578 Å and 3927.7–3939.7 Å.[94] The four fixed points of the black polygon are (2.683, 5.1), (3.59, 5.1), (6.071, −0.357), (2.279, 2.676).

The periods and some physic parameters of exotic stars can be figured out by the spectra of TD observation. According to the understanding variable stars[52] and other catalogs, we compiled a catalog (hereafter, we name it exotic star catalog) with 112554 exotic stars which include Be stars, cataclysmic variable stars, classical cepheid stars, x-ray binaries, symbiotic stars and so on (see Table 3, the catalog is available in Science Data Bank).

Table 2. The priority of input source. The second column is the priority of input sources in the first year (201810–201907). The third and last columns are for plates located close to the galactic disk and at the high galactic latitude, respectively (see 12 blue and two purple plates of Fig. 3). G_{OBWD} stands for O-, B-, WD and sdOB selected from *Gaia* CMD ($10 \le G < 14.5$, without correcting color and extinction). ! indicates the source without observation. S_{18-19} denotes star observed in the first year of LAMOST-MRS; SE means the stars in our exotic stars catalog (see Table 3); SE_{18-19} stands for the exotic star observed in the first year of LAMOST-MRS. LFeH stands for the low-metallicity candidate selected by line indices of Hα and CaII K (see Fig. 5).

Priority	201810–201907	(LGL plates) 201910–	(HGL plates) 201910–
1	G_{OBWD}	SE_{18-19}	LFeH & ($10 \le G < 14.5$)
2	GALEX & ($10 \le G < 13$)	!SE_{18-19} & ($10 \le G < 14.5$)	SE & ($10 \le G < 14.5$)
3	!GALEX & ($10 \le G < 12$)	S_{18-19} & LFeH	G_{OBWD}
4	!GALEX & ($12 \le G < 13$)	rest LFeH & ($10 \le G < 14.5$)	GALEX & ($10 \le G < 13$)
5	GALEX & ($13 \le G < 14$)	rest S_{18-19}	!GALEX & ($10 \le G < 12$)
6	GALEX & ($14 \le G < 14.5$)	rest G_{OBWD}	!GALEX & ($12 \le G < 13$)
7	!GALEX & ($13 \le G < 14$)	rest GALEX & ($10 \le G < 13$)	GALEX & ($13 \le G < 14$)
8	!GALEX & ($14 \le G < 14.5$)	rest !GALEX & ($10 \le G < 12$)	GALEX & ($14 \le G < 14.5$)
9		rest !GALEX & ($12 \le G < 13$)	!GALEX & ($13 \le G < 14$)
10		rest GALEX & ($13 \le G < 14$)	!GALEX & ($14 \le G < 14.5$)
11		rest GALEX & ($14 \le G < 14.5$)	
12		rest !GALEX & ($13 \le G < 14$)	
13		rest !GALEX & ($14 \le G < 14.5$)	

Table 3. Catalogue name of exotic stars (their coordinates can be found in Science Data Bank, Catalog 2). N_{star} denotes the number of stars in the MRS-B field of DR8 which accumulates all LAMOST-MRS spectra observed from 2017-09-19 to 2020-05-27.

Name	Brief description	N_{star}	References
Be_{HIPP}	Be star in the HIPPARCOS	0	[53]
CV	cataclysmic variables	0	[54]
Cepheid	classical cepheid stars	1	[55,56]
EB_{Algol}	eclipsing binaries with algol-type light curve	2	[57,58]
EB_{Xray}	eclipsing binaries with x-ray	2	[59–61]
GCVS5	the general catalogue of variable stars: Version GCVS 5.1	149	[56]
γDor	γ Doradus variable stars	0	[62–64]
γRay	γ-ray burst pulses	0	[65–68]
Herbig	Herbig Ae Be stars	6	[69–71]
LumStar	photometry and spectroscopy for luminous stars	168	[72]
OB	O- and B-type stars	1851	[73,74]
RCB	the R coronae Borealis stars	0	[75–77]
RRLyrae	RR Lyrae stars	1	[78]
RotateVB	rotational variable stars	0	[79–83]
SB	spectroscopy binaries	0	[84]
SySt	symbiotic stars	0	[85,86]
TTauri	T Tauri stars	6	[87,87]
UVCeti	the UV Cet-type flare stars	0	[88]
WD+FKG	WD+FKG-type binaries	6	[89]
WR	Wolf Rayet stars	1	[90–92]
δ Scuti	δ Scuti stars	5	[93]

Although close binary fraction decreases with metallicity proved by the recent research,[20,33] it is still unclear whether the relation is universal for all primary stars. However, the low-metallicity ($[Fe/H] < -1$) stars are rare. We pick out the low-metallicity candidates from LAMOST-LRS spectra of DR6 by using the diagram of line indices of Hα and CaII K. The index band-pass of the line indices can be found in Table 2 of Liu *et al.* (2015).[94] From Fig. 5, we can see that low-metallicity stars are concentrated at a specific region in the diagram of line indices of Hα and CaII K. We roughly selected the sources located in the black polygon as our low-metallicity candidates.

Since the identified exotic stars and low-metallicity stars are rare, we increased their priorities in the following observations. Then we gave the observed sources high priorities to guarantee that we would observe plenty of stars with > 10 visits (see Table 2).

5. Parameter determination and analysis

Raw CCD data were reduced by the LAMOST 2D pipeline. The procedures of extracting 1D spectra from 2D images include dark and bias subtraction, spectral extraction, sky subtraction and wavelength calibration. The procedures are the same as those of the 2D pipeline used by the LAMOST-LRS,[95] except that the wavelength calibration is based on Th-Ar or Sc lamps without stacking of subexposures.[36] The SNRs of all pixels were calculated, and the medians were taken as the final values for blue (SNR_B) and red (SNR_R) arms of each spectrum. The eighth year survey data has been released, which includes LAMOST-MRS spectra observed from

September 2018 to Jun 2020 (DR8-MRS). There are 53360 sources observed in MRS-B field, but SNR_B and SNR_R of some sources are both zeros due to the bad fibers or weather conditions. We picked out 731752 spectra with $SNR_B > 5$ or $SNR_R > 5$ that belong to 49129 sources of MRS-B. Cross-matching the sources with DR8-MRS by the sky separation of 5″, we obtain 892233 spectra with $SNR_B > 5$ or $SNR_R > 5$, because some of the sources are observed by the other sub-surveys of LAMOST-MRS (such as NT survey) as well. We get 28828 and 3375 sources that are visited ≥ 2 and ≥ 10 times, which have at least a $SNR_B \geq 10$ spectrum in each visit.

5.1. Atmospheric parameters

The stellar parameters are from the LAMOST pipeline, i.e., LASP, which adopts the ELODIE library as templates. The templates are interpolated with a polynomial spectral model and then downgraded to LAMOST spectral resolution automatically while matching to observations.[96] In DR8, the published LAMOST MRS stellar parameters are derived from the stacked spectra from multi-epoch spectra of the blue arm obtained in one night. Zong *et al.* (2020) found that the uncertainties of $T_{\rm eff}$, $\log g$ and [Fe/H] are 100 K, 0.15 dex and 0.09 dex, respectively,[39] by comparing the common sources observed by *Gaia*[97] and the Apache Point Observatory Galactic Evolution Experiment (APOGEE)[26,98] in the MRS-K field. There are 36516 sources in the MRS-B field that have atmospheric parameters derived by LASP.

A few contamination of early-type spectra can be found, as shown by the blue dots in Figs. 6(a) and 6(b). Some early-type stars with corrected $G_{\rm BP} - G_{\rm RP} < 0.1$ would be mistaken as metal-poor stars with temperature $T_{\rm eff} \sim 6000$ K. Because the LASP could only provide parameters for stars with spectral types of late A-, F-, G-, and K-type due to the limitation of templates library. The early-type stars, especially O- and B-type stars barely have metal lines in the blue arm spectra which thus make them look like poor metal-poor stars.

Guo *et al.* (2021) picked out early-type stars from DR7 and selected the best SNR epoch spectra to measure the atmospheric parameters by using the Stellar LAbel Machine (SLAM).[99,100] We find that 1718 early-type stars of MRS-B field are in their Table 2 that atmospheric parameters were

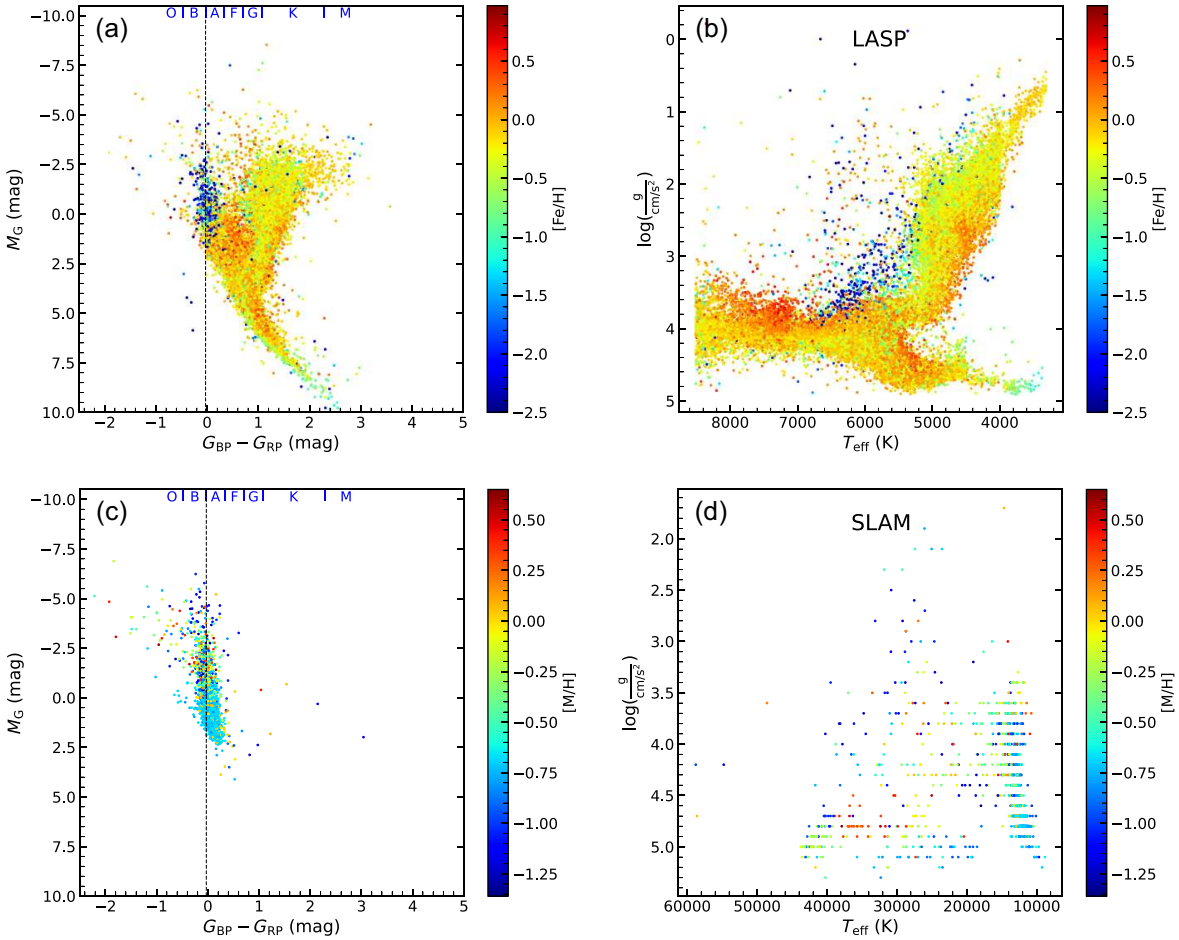


Fig. 6. The CMD and Kiel diagram colored by [Fe/H] or [M/H]. The upper rows show the stars with atmosphere parameters derived by the updated LASP pipeline, the median values are used for the source with multiple spectra. The bottom rows show the early-type stars with parameters measured with the best SNR spectra by using SLAM. Since the uncertainty is about 0.29 dex, only one decimal place is saved, so that the $\log g$ in panel (b) is waffle-like. Note that: [M/H] is the abundance of elements present in an object that are heavier than hydrogen and helium; [Fe/H] is the iron abundance, we use [Fe/H] to stand for metallicity abundance if there is no specific statement. Caution: there are two stars (obsid: 727414208, 681809175) with $T_{\rm eff} > 55000$ K, which are misled by the features of SB2.

derived by using LAMOST-MRS spectra. According to their analysis, the uncertainties of $T_{\rm eff}$ and $\log g$ are 2,185 K and 0.29 dex; the metallicity abundance [M/H] cannot be constrained very well with LAMOST-MRS spectra (details see the bottom-left panel of their figure 9). There are two stars (see Fig. 6(d), obsid: 727414208, 681809175) with $T_{\rm eff} > 55000$ K which are out of the training grid of SLAM (10000–55000 K). We find that their spectra have features of SB2 checked by eyes, which misled the measurements of the effective temperature.

5.2. Stellar type

There is a gap (8500 K $< T_{\rm eff} <$ 10000 K) between the $T_{\rm eff}$ derived by the LASP and the SLAM, and the atmospheric parameters are not derived for all of the sources in the MRS-B filed. For the sake of simplicity and uniformity, we choose *Gaia* CMD to coarsely identify which types the sources belong to (see Fig. 4). We correct the color and magnitude induced by interstellar dust. The color excess $E(B-V)$ is obtained by using the median value of the Bayestar 3D dust maps of *dustmaps*[51] with the galactic coordinates, parallax of *Gaia* EDR3,[101] and the distance is simply derived by dividing the parallax ($d = 1/\varpi$). Then the color excess $E(G_{\rm BP}-G_{\rm RP})$ and extinction A_G are calculated with the following equations:

$$E(G_{\rm BP}-G_{\rm RP}) = (1.002-0.589)\frac{E(B-V)}{0.317}, \quad (1)$$

$$A_G = 0.789\frac{E(B-V)}{0.317}, \quad (2)$$

where the coefficient are relative extinction values of Table 3 of Wang *et al.* (2019).[102]

There are 49078 stars with available color index $G_{\rm BP}-G_{\rm RP}$ and parallaxes. We can see that majority of the stars are MS and red clump stars (RCs), and F-type dwarf stars are maximum which contain 7927 sources with $N_{\rm vist} \geq 2$ and each visit has at least a spectrum of ${\rm SNR_B} \geq 10$ (hereafter, $N_{\rm vist} \geq 2$ denotes the number of stars that have been visited more than twice and have at least spectrum of ${\rm SNR_B} \geq 10$ in each visit without specification explanation). More than 1500 sources are observed with $N_{\rm vist} \geq 2$ for each of B-, A-, F-, and G-type MSs (for details see Table 5). We coarsely select MS star by using the black polygon of Fig. 4, since it does not influence the statistical result so much. Giant stars can be observed in a larger volume than the volume of dwarf stars because LAMOST-MRS-B only observes the stars with apparent magnitude from 10 mag to 15 mag. So that most G- and K-type stars are giants and located in the region of the RC star (see Fig. 4), as shown in Fig. 7(a). We can see that K- and M-type dwarfs are less; G-type dwarfs are even less numerous than F-type (see Fig. 7(a) and Table 5) because we prefer to observe brighter stars to obtain higher SNRs.

Although the highest observation priorities are given to the exotic stars, only few of them have been observed. As the orange curves shown in Fig. 4, we select WD and sdOB. Only one WD (J041010.32+180223.8) is observed and cannot even see in the 2D histogram of the CMD. It is faint with $G = 11.42$ mag, ${\rm SNR_B} = 7.14$ and ${\rm SNR_R} = 5.24$. Nine sdOB are observed one of which has been visited 10 times. WD and sdOB are too faint or rare to be observed. Eliminating O- and B-type stars, 347 stars of the exotic star catalog are (see Table 3) in the MRS-B of DR8, which include a Wolf Rayet star (HD 195177) and two high mass x-ray binaries (IGR J06074+2205 and HD 249179).

The low [Fe/H] candidates also have high observation priorities. Excluding the contamination of O- and B-type stars ($G_{\rm BP}-G_{\rm RP} < 0.1$), we have only 276 stars with [Fe/H] < -1 dex. It is hard to obtain the statistic property of binary orbital parameters for the metal-poor stars. As shown in Fig. 7(b), most stars are distributed in the interval of $-0.6 <$ [Fe/H] < 0.4 dex. Thousands of them are observed more than twice. There are two stars with [Fe/H] > 0.8. Note: the derived [Fe/H] might be wrong for the the metal-richest and metal-poorest.

Table 4. The numbers of observed stars in different types. MS means the main sequence star. $N_{\rm vist} \geq 2$ stands for the number of stars which are visited more than twice and have at least a ${\rm SNR_B} \geq 10$ spectrum in each visit. There are 49078 sources that have parallax and $G_{\rm BP}-G_{\rm RP}$ of *Gaia*.

TYPE	O	B	A	F	G	K	M
$G_{\rm BP}-G_{\rm RP}$	< -0.3	$(-0.3, 0.1)$	$(0.1, 0.5)$	$(0.5, 0.8)$	$(0.8, 1.2)$	$(1.2, 2.4)$	> 2.4
All	314	3880	9610	13068	12511	9071	624
MS	188	3859	9441	12688	5354	1011	40
All ($N_{\rm visit} \geq 2$)	245	2725	6203	7927	7280	4752	193
MS ($N_{\rm visit} \geq 2$)	143	2711	6091	7680	3083	462	2

Table 5. The numbers of observed stars in different types. MS means the main sequence star. $N_{\rm vist} \geq 2$ stands for the number of stars which are visited more than twice and have at least a ${\rm SNR_B} \geq 10$ spectrum in each visit. There are 49078 sources that have parallaxes and $G_{\rm BP}-G_{\rm RP}$ of *Gaia* EDR3.

TYPE	O	B	A	F	G	K	M
$G_{\rm BP}-G_{\rm RP}$ (mag)	< -0.48	$[-0.48, -0.03)$	$[-0.03, 0.33)$	$[0.33, 0.71)$	$[0.71, 1.07)$	$[1.07, 2.28)$	≥ 2.28
All	174	1523	7794	13218	11641	13984	746
MS	53	1511	7716	12944	8883	1547	64
All ($N_{\rm visit} \geq 2$)	140	1177	5377	8740	7329	8010	262
MS ($N_{\rm visit} \geq 2$)	41	1171	5314	8565	5562	843	8

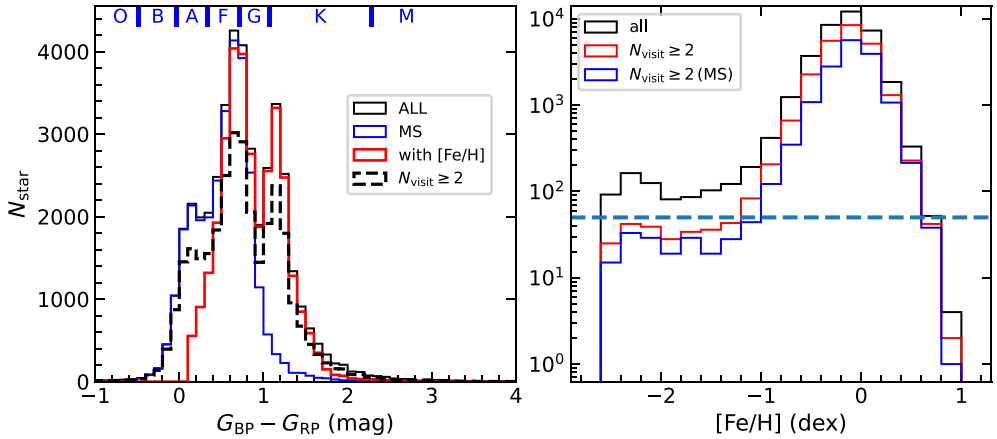


Fig. 7. (a) The histogram of stars which have at least a spectrum of $SNR_B \geq 10$ in each visit. MS stands for main sequence star. $G_{BP} - G_{RP}$ is corrected by using *dustmaps*. The ordinate axis of (b) is in a logarithmic scale to make the small numbers visible at poor and rich metallicity bins.

We compile a catalog that includes RVs, stellar atmospheric parameters derived by LASP and SLAM, information of exotic stars, and a few columns of LAMOST and *Gaia* such as *obsid*, *mjd*, *parallax* and *source_id*, for the 892233 spectra (the catalog is available in Science Data bank).

5.3. Visit and repeat rates

We prefer to counts the stars that have at least a $SNR_B \geq 10$ spectrum in each visit, which would obtain reliable RVs. There are totally 42193 sources with at least a $SNR_B \geq 10$ spectrum, and 31073 sources are visited more than twice. From Fig. 8, we can see that most of the stars were visited 2–5 times, and 2735 sources have been visited more than 10 times. It is hard to obtain good SNRs for all of the stars in each visit. For example, there are 1713 sources in the TD114941N345554B01 plate that have been visited 15 times, while only 287 (17%) sources are visited 15 times with $SNR_B \geq 10$. The stars that are observed with time span of > 700 days came from the test plates of LAMOST-MRS pilot program such as HIP28117, which has the same center coordinates as TD055633N285632B01. Though we set three exposures per visit in the observation, a large fraction (28589) of stars were observed with more exposures (see Fig. 8(a)) which profits from observations of the other sub-surveys. It would be useful to, but is not restricted to, study the binaries with periods less than one day.

After the first year of observation of LAMOST-MRS, we kept 12 plates to observe and modified the observation priorities of their input sources. The repeat rate can be estimated by using the night plates observed in the second year. From Fig. 9, we can see that more than 70% of the sources are left for all plates. We lost 5149 stars observed more than twice without considering the plate of TD043724N254338, which would be observed in the MRS-S field and has a similar priority to MRS-B field (the second and following years). The plate HIP28117 was visited five times from 2017-10-29 to 2017-11-08, and 1747 sources were observed of which 516 stars are still observed in the TD055633N285632B01.

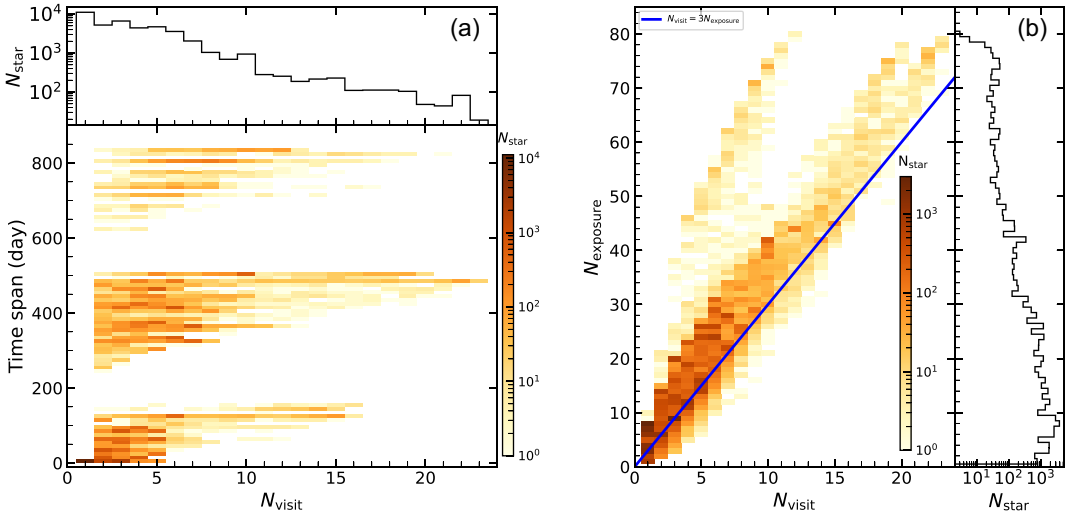


Fig. 8. (a) The distribution of the number of visits and the time span of the stars observed in DR8 of MRS-B field, and there is at least a spectrum with $SNR_B \geq 10$ in each visit. (a) The distribution of the numbers of visits and exposures, and the spectrum of each exposure has $SNR_B \geq 10$.

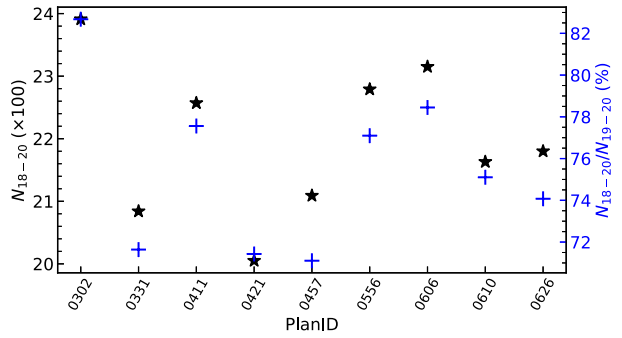


Fig. 9. The repeat rate of plates observed from October 2018 to June 2020. N_{18-19} and N_{19-20} denote the numbers of stars observed from October 2018 to July 2019 and October 2019 to June 2020, respectively. The detail number can be found in Table 1.

There are 34107 sources that have been observed more than twice with $\mathrm{SNR_B} > 5$ or $\mathrm{SNR_R} > 5$ in MRS-B. We subtract the abandoned sources (5149+1231) which have been observed more than twice, and the remaining 27727 sources will be observed in the next few years. There are still 3 plates that are not observed in the second year (see Table 1). Two of them were only visited one time in the first year, so that 5000 sources would be observed in the following years. We would obtain over 30000 sources that have the potential to be visited more than 10 times. We can get more visits as considering the common sources that might be observed in the other sub-survey fields of LAMOST-MRS.

5.4. Radial velocity

We measure the self-consistent stellar RV,[36] which reduces the temporal variation of the RV zero-points (between exposures) by combining LAMOST-MRS with *Gaia* EDR3.[101] We find that $> 95\%$ spectra with $\mathrm{SNR_B} \geq 10$ have $\sigma_{\mathrm{rv}} < 10\ \mathrm{km \cdot s^{-1}}$ in the MRS-B field. Comparing the cumulative density functions (CDF) of $\sigma_{\mathrm{rv}}^{\mathrm{B}}$ and $\sigma_{\mathrm{rv}}^{\mathrm{R}}$, we find that CDF of $\sigma_{\mathrm{rv}}^{\mathrm{B}}$ is steeper when $\sigma_{\mathrm{rv}} < 1\ \mathrm{km \cdot s^{-1}}$, as the thick lines of Fig. 10 shown, but CDF of $\sigma_{\mathrm{rv}}^{\mathrm{R}}$ is steeper when $\sigma_{\mathrm{rv}} > 1\ \mathrm{km \cdot s^{-1}}$. Then, we divide the spectra into two sets by the corrected color $G_{\mathrm{BP}} - G_{\mathrm{RP}} = 0.5$ of the stars. From the blue and red thin lines of Fig. 10, we can see that CDF of $\sigma_{\mathrm{rv}}^{\mathrm{R}}$ is steeper for early-type stars ($G_{\mathrm{BP}} - G_{\mathrm{RP}} < 0.5$), while the situation is inverse for the late-type stars ($G_{\mathrm{BP}} - G_{\mathrm{RP}} > 0.5$, see the dashed lines). It indicates that the RVs derived by the red arm spectra are preciser than the RVs of blue arm spectra for early-type stars due to that the absorption lines of early-type stars are weak and rare in the blue arm spectra. In addition, for the late-type stars, $> 95\%$ spectra have $\sigma_{\mathrm{rv}} < 1\ \mathrm{km \cdot s^{-1}}$.

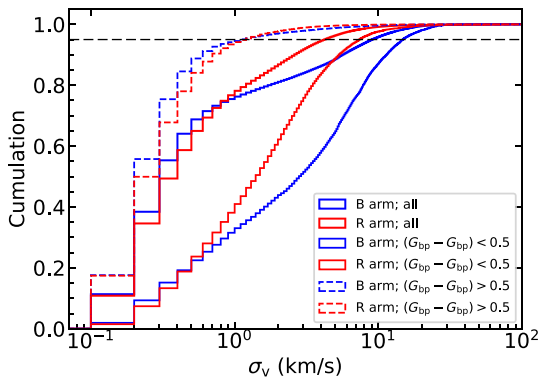


Fig. 10. The cumulative density function of RV uncertainties of the spectra with $\mathrm{SNR_B} \geq 10$. Blue and red colors stand for RV uncertainties measured from blue and red arm spectra, respectively. $G_{\mathrm{BP}} - G_{\mathrm{RP}}$ is corrected by using *dustmaps*. The black dashed line stands for 95%.

6. Summary and prospective

After the first five years survey of LAMOST-LRS, LAMOST-MRS had been started regularly since 2018. We obtain about 20% observation time to study the properties of close binary and exotic stars. We initially input 25 plates in the first year, and 16 plates were observed and 34 visits were obtained. It is difficult to observe all the plates with > 10 visits in the next four years. So we dropped out 13 of them and added two new plates located at the high galactic latitude. Checking the second year observation, we get 61 visits, of which 29 visits are from the two high galactic latitude plates. We would achieve our goals to obtain about 30000 sources with $N_{\mathrm{vist}} \geq 2$ by estimating the number of the visits during the 2-year observation. We might obtain more visits due to the common sources observed by the other sub-surveys of LAMOST-MRS.

We placed our plates a little away from the galactic disk plane in order to pick out the exotic objects composited of WD+MS stars and reduce their influence on the statistic property of binary by using the UV catalog of GLAEX. We gave some identified exotic objects with the highest observation priorities, and DR8 include 347 the identified exotic objects in the MRS-B field. These objects could be well studied with LAMOST-MRS spectra. For example, we could study the variation of Hα emission line of $\mathrm{EB_{Xray}}$ and WR, or obtain orbital parameters of WD+FKG binaries. In addition, a few exotic objects ($\sim 1\%$) will not influence the process of analyzing the statistical properties of binary.

We also set high observation priorities for the low metallicity candidates. We found that there are about 200 sources with $[\mathrm{Fe/H}] < -1$ dex after checking DR8. It is possible to analyze the binary fraction of these metal-poor stars. For the source with $-0.6 < [\mathrm{Fe/H}] < 0.4$, we might be able to study the correlation between binary orbital parameters and metallicity abundance by using the all 5-year data, since there are > 1000 sources in each of 0.2 dex bins.

There are 53360 sources in the MRS-B filed, of which 28828 and 3375 sources are visited ≥ 2 and ≥ 10 times, which have at least one $\mathrm{SNR_B} \geq 10$ spectrum in each visit. We gave the brighter sources with higher observation priorities so that most of the observation stars belong to F-type, and majority of G- and K-type stars are located in the region of RC star. Each number of B-, A-, F-, and G-type dwarfs is more than 1500,

these will give us an opportunity to obtain precise values of close binary fraction for the different type stars. By the way, the RV precisions of early- and late-type stars are better than $1\,\mathrm{km\cdot s^{-1}}$ and $10\,\mathrm{km\cdot s^{-1}}$, respectively. Therefore, it becomes possible to study the binary statistic properties in smaller stellar mass bins and obtain more reliable relations between the orbital parameters.

In addition, we are also trying to use a few visits data of LAMOST-MRS to find exotic stars and study binarity. By using LAMOST-MRS DR7, we identified 1162 Be stars[103] and a quadruple (2+2) system which is the most massive eclipse quadruple system ever found (in preparation, Li *et al.*). We found that the $f_{\rm b}$ varies from about 68% to 44% with stellar spectral type varied from B- to A-type.[104] The power law index of mass ratio distribution (γ) changes from -0.42 ± 0.27 to 2.12 ± 0.19 when the spectral type varies from A- to G-type by analyzing the SB2 stars.[105] We will resolve the orbital periods of the stars with the full 5-year observation and release them.

All the datasets presented in this paper, including the two catalogs and descriptions, are compiled in the supplementary materials.

Data availability statement

The data that support the findings of this study are openly available in Science Data Bank at http://www.doi.org/10.57760/sciencedb.j00113.00035

Acknowledgements

The authors thank Jian-Ning Fu, Xiao-Jie Xu, Yin-Bi Li, Zhong-Rui Bai and all of members of LAMOST-MRS Working Group for valuable discussions. This work is supported by the National Natural Science Foundation of China (Grant Nos. 12073070, 12173081, 12090043, 11873016, and 12173013), Yunnan Fundamental Research Project (Grant No. 202101AV070001), the Science Research Grants from The China Manned Space Project (Grant Nos. CMS-CSST-2021-A08, CMS-CSST-2021-A10, and CMS-CSST-2021-B05) and CAS 'Light of West China' Program.

Guoshoujing Telescope (the Large Sky Area Multi-Object Fiber Spectroscopic Telescope LAMOST) is a National Major Scientific Project built by the Chinese Academy of Sciences. Funding for the project has been provided by the National Development and Reform Commission of China. LAMOST is operated and managed by the National Astronomical Observatories, Chinese Academy of Sciences.

This work has made use of data from the European Space Agency (ESA) mission *Gaia*, processed by the *Gaia* Data Processing and Analysis Consortium (DPAC). Funding for the DPAC has been provided by national institutions, in particular the institutions participating in the *Gaia* Multilateral Agreement.

The LAMOST fellowship is supported by Special Funding for Advanced Users, budgeted and administrated by Center for Astronomical Mega-Science, Chinese Academy of Sciences (CAMS). This work is supported by Cultivation Project for LAMOST Scientific Payoff and Research Achievement of CAMS-CAS and Special Research Assistant Program of Chinese Academy of Sciences.

Software: python, laspec,[100] astropy,[106] TOPCAT.[107]

References

[1] Duchêne G and Kraus A 2013 *ARA&A* **51** 269
[2] Moe M and Di Stefano R 2017 *ApJS* **230** 15
[3] Offner S S R, Moe M, Kratter K M, Sadavoy S I, Jensen E L N and Tobin J J. 2022 arXiv e-prints arXiv: 2203.10066
[4] Fuhrmann K and Chini R 2012 *ApJS* **203** 30
[5] Tokovinin A 2014 *AJ* **147** 86
[6] Sana H, de Mink S E, de Koter A, Langer N, Evans C J, Gieles M, Gosset E, Izzard R G, Le Bouquin J B and Schneider F R N 2012 *Science* **337** 444
[7] Han Z W, Ge H W, Chen X F and Chen H L 2020 *Research in Astronomy and Astrophysics* **20** 161
[8] Mohamed S and Podsiadlowski P 2012 *Baltic Astronomy* **21** 88
[9] Mikołajewska J 2012 *Baltic Astronomy* **21** 5
[10] Belczynski K 2020 *ApJ* **905** L15
[11] Burstein D, Bertola F, Buson L M, Faber S M and Lauer T R 1988 *ApJ* **328** 440
[12] Han Z, Podsiadlowski P and Lynas-Gray A E 2007 *MNRAS* **380** 1098
[13] Chen H L, Woods T E, Yungelson L R, Gilfanov M and Han Z 2015 *MNRAS* **453** 3024
[14] Secunda A, Cen R, Kimm T, Götberg Y and de Mink S E 2020 *ApJ* **901** 72
[15] Götberg Y, de Mink S E, McQuinn M, Zapartas E, Groh J H and Norman C 2020 *A&A* **634** A134
[16] Sana H, Le Bouquin J B, Lacour S, Berger J P, Duvert G, Gauchet L, Norris B, Olofsson J, Pickel D, Zins G, Absil O, de Koter A, Kratter K, Schnurr O and Zinnecker H 2014 *ApJS* **215** 15
[17] Raghavan D, McAlister H A, Henry T J, Latham D W, Marcy G W, Mason B D, Gies D R, White R J and ten Brummelaar T A 2010 *ApJS* **190** 1
[18] Winters J G, Henry T J, Jao W C, Subasavage J P, Chatelain J P, Slatten K, Riedel A R, Silverstein M L and Payne M J 2019 *AJ* **157** 216
[19] Kobulnicky H A, Chick W T, Schurhammer D P, Andrews J E, Povich M S, Munari S A, Olivier G M, Sorber R L, Wernke H N, Dale D A and Dixon D M 2016 *ApJS* **227** 18
[20] Moe M, Kratter K M and Badenes C 2019 *ApJ* **875** 61
[21] Latham D W, Stefanik R P, Torres G, Davis R J, Mazeh T, Carney B W, Laird J B and Morse J A 2002 *AJ* **124** 1144
[22] Moe M and Di Stefano R 2013 *ApJ* **778** 95
[23] Carney B W 1983 *AJ* **88** 623
[24] Abt H A and Willmarth D W 1987 *ApJ* **318** 786
[25] Hettinger T, Badenes C, Strader J, Bickerton S J and Beers T C 2015 *ApJ* **806** L2
[26] Majewski S R, Schiavon R P, Frinchaboy P M, *et al.* 2017 *AJ* **154** 94
[27] Cui X Q, Zhao Y H, Chu Y Q, *et al.* 2012 *Research in Astronomy and Astrophysics* **12** 1197
[28] Zhao G, Zhao Y H, Chu Y Q, Jing Y P and Deng L C 2012 *Research in Astronomy and Astrophysics* **12** 723
[29] Gao S, Liu C, Zhang X, Justham S, Deng L and Yang M 2014 *ApJ* **788** L37
[30] Gao S, Zhao H, Yang H and Gao R 2017 *MNRAS* **469** L68
[31] Tian Z J, Liu X W, Yuan H B, Chen B Q, Xiang M S, Huang Y, Wang C, Zhang H W, Guo J C, Ren J J, Huo Z Y, Yang Y, Zhang M, Bi S L, Yang W M, Liu K, Zhang X F, Li T D, Wu Y Q and Zhang J H 2018 *Research in Astronomy and Astrophysics* **18** 052
[32] Badenes C, Mazzola C, Thompson T A, *et al.* 2018 *ApJ* **854** 147
[33] Mazzola C N, Badenes C, Moe M, *et al.* 2020 *MNRAS* **499** 1607

[34] Liu C 2019 *MNRAS* **490** 550
[35] Liu C, Fu J, Shi J, *et al.* 2020 arXiv e-prints arXiv:2005.07210
[36] Zhang B, Li J, Yang F, Xiong J P, Fu J N, Liu C, Tian H, Li Y B, Wang J X, Liang C X, Zhou Y T, Zong W, Yang C Q, Liu N and Hou Y H 2021 *ApJS* **256** 14
[37] Valenti J A, Piskunov N and Johns-Krull C M 1998 *ApJ* **498** 851
[38] Fu J N, Cat P D, Zong W, Frasca A, Gray R O, Ren A B, Molenda-Żakowicz J, Corbally C J, Catanzaro G, Shi J R, Luo A L and Zhang H T 2020 *Research in Astronomy and Astrophysics* **20** 167
[39] Zong W, Fu J N, De Cat P, Wang J, Shi J, Luo A, Zhang H, Frasca A, Molenda-Żakowicz J, Gray R O, Corbally C J, Catanzaro G, Cang T, Wang J, Chen J, Hou Y, Liu J, Niu H, Pan Y, Tian H, Yan H, Zhang Y and Zuo H 2020 *ApJS* **251** 15
[40] Wu C J, Wu H, Zhang W, Ren J J, Chen J J, Hsia C H, Wu Y Z, Zhu H, Li B, Hou Y H, Wang J L, Yu S R, Yu S R and Lamost Mrs Collaboration 2021 *Research in Astronomy and Astrophysics* **21** 096
[41] Marconi M, Bono G, Caputo F, Piersimoni A M, Pietrinferni A and Stellingwerf R F 2011 *ApJ* **738** 111
[42] Jurcsik J, Smitola P, Hajdu G, Sódor Á, Nuspl J, Kolenberg K, Fűrész G, Balázs L G, Pilachowski C, Saha A, Moór A, Kun E, Pál A, Bakos J, Kelemen J, Kovács T, Kriskovics L, Sárneczky K, Szalai T, Szing A and Vida K 2017 *MNRAS* **468** 1317
[43] Price-Whelan A M, Hogg D W, Foreman-Mackey D and Rix H W 2017 *ApJ* **837** 20
[44] Price-Whelan A M, Hogg D W, Rix H W, De Lee N, Majewski S R, Nidever D L, Troup N, Fernández-Trincado J G, García-Hernández D A, Longa-Peña P, Nitschelm C, Sobeck J and Zamora O 2018 *AJ* **156** 18
[45] Wolff S C 1978 *ApJ* **222** 556
[46] Garmany C D, Conti P S and Massey P 1980 *ApJ* **242** 1063
[47] Shao Y and Li X D 2020 *ApJ* **898** 143
[48] Hurley J R, Tout C A and Pols O R 2002 *MNRAS* **329** 897
[49] Belczynski K, Kalogera V, Rasio F A, Taam R E, Zezas A, Bulik T, Maccarone T J and Ivanova N 2008 *ApJS* **174** 223
[50] Bianchi L, Shiao B and Thilker D 2017 *ApJS* **230** 24
[51] Green G M, Schlafly E, Zucker C, Speagle J S and Finkbeiner D 2019 *ApJ* **887** 93
[52] Percy J R 2007 *Understanding Variable Stars* 2007 (Cambridge: Cambridge University Press)
[53] Hubert A M and Floquet M 1998 *A&A* **335** 565
[54] Downes R A, Webbink R F, Shara M M, Ritter H, Kolb U and Duerbeck H W 2001 *PASP* **113** 764
[55] Szabados L 2003 *Information Bulletin on Variable Stars* **5394** 1
[56] Samus' N N, Kazarovets E V, Durlevich O V, Kireeva N N and Pastukhova E N 2017 *Astronomy Reports* **61** 80
[57] Budding E, Erdem A, Çiçek C, Bulut I, Soydugan F, Soydugan E, Bakiş V and Demircan O 2004 *A&A* **417** 263
[58] Papageorgiou A, Catelan M, Christopoulou P E, Drake A J and Djorgovski S G 2018 *ApJS* **238** 4
[59] Liu Q Z, van Paradijs J and van den Heuvel E P J 2000 *A&AS* **147** 25
[60] Liu Q Z, van Paradijs J and van den Heuvel E P J 2006 *A&A* **455** 1165
[61] Liu Q Z, van Paradijs J and van den Heuvel E P J 2007 *A&A* **469** 807
[62] Hauck B and Mermilliod M. 1990 *A&AS* **86** 107
[63] Handler G. 1995 *Information Bulletin on Variable Stars* **4216** 1
[64] Krisciunas K and Handler G. 1995 *Information Bulletin on Variable Stars* **4195** 1
[65] Gruber D, Goldstein A, Weller von Ahlefeld V, *et al.* 2014 *ApJS* **211** 12
[66] von Kienlin A, Meegan C A, Paciesas W S, *et al.* 2014 *ApJS* **211** 13
[67] Narayana Bhat P, Meegan C A, von Kienlin A, *et al.* 2016 *ApJS* **223** 28
[68] Hakkila J, Horváth I, Hofesmann E and Lesage S 2018 *ApJ* **855** 101
[69] The P S, de Winter D and Perez M R. 1994 *A&AS* **104** 315
[70] Herbst W and Shevchenko V S 1999 *AJ* **118** 1043
[71] Vioque M, Oudmaijer R D, Baines D, Mendigutía I and Pérez-Martínez R 2018 *A&A* **620** A128
[72] Reed B C 2005 *AJ* **130** 1652
[73] Almeida L A, Sana H, Taylor W, *et al.* 2017 *A&A* **598** A84
[74] Liu Z, Cui W, Liu C, Huang Y, Zhao G and Zhang B 2019 *ApJS* **241** 32
[75] Clayton G C 1996 *PASP* **108** 225
[76] Montiel E J, Clayton G C, Sugerman B E K, Evans A, Garcia-Hernández D A, Kameswara Rao N, Matsuura M and Tisserand P 2018 *AJ* **156** 148
[77] Feast M W, Griffin R F, Herbig G H and Whitelock P A 2019 *MNRAS* **482** 4174
[78] Maintz G 2005 *A&A* **442** 381
[79] Manchester R N, Hobbs G B, Teoh A and Hobbs M 2005 *AJ* **129** 1993
[80] Eker Z, Ak N F, Bilir S, Doğru D, Tüysüz M, Soydugan E, Bakış H, Uğraş B, Soydugan F, Erdem A and Demircan O 2008 *MNRAS* **389** 1722
[81] Renson P and Manfroid J 2009 *A&A* **498** 961
[82] Zechmeister M, Kürster M, Endl M, Lo Curto G, Hartman H, Nilsson H, Henning T, Hatzes A P and Cochran W D 2013 *A&A* **552** A78
[83] Boro Saikia S, Marvin C J, Jeffers S V, Reiners A, Cameron R, Marsden S C, Petit P, Warnecke J and Yadav A P 2018 *A&A* **616** A108
[84] Gullikson K, Kraus A, Dodson-Robinson S, Jaffe D, Lee J E, Mace G N, MacQueen P, Park S and Riddle A 2016 *AJ* **151** 3
[85] Li J, Mikołajewska J, Chen X F, Luo A L, Rebassa-Mansergas A, Hou Y H, Wang Y F, Wu Y, Yang M, Zhang Y and Han Z W 2015 *Research in Astronomy and Astrophysics* **15** 1332
[86] Akras S, Guzman-Ramirez L, Leal-Ferreira M L and Ramos-Larios G 2019 *ApJS* **240** 21
[87] Galli P A B, Bertout C, Teixeira R and Ducourant C 2015 *A&A* **580** A26
[88] Gershberg R E, Katsova M M, Lovkaya M N, Terebizh A V and Shakhovskaya N I 1999 *A&AS* **139** 555
[89] Rebassa-Mansergas A, Ren J J, Irawati P, *et al.* 2017 *MNRAS* **472** 4193
[90] Smith L F 1968 *MNRAS* **138** 109
[91] van der Hucht K A 2001 *New A Rev.* **45** 135
[92] Rosslowe C K and Crowther P A 2015 *MNRAS* **447** 2322
[93] Chang S W, Protopapas P, Kim D W and Byun Y I 2013 *AJ* **145** 132
[94] Liu C, Cui W Y, Zhang B, Wan J C, Deng L C, Hou Y H, Wang Y F, Yang M and Zhang Y 2015 *Research in Astronomy and Astrophysics* **15** 1137
[95] Luo A L, Zhao Y H, Zhao G, *et al.* 2015 *Research in Astronomy and Astrophysics* **15** 1095
[96] Wu Y, Luo A L, Li H N, Shi J R, Prugniel P, Liang Y C, Zhao Y H, Zhang J N, Bai Z R, Wei P, Dong W X, Zhang H T and Chen J J 2011 *Research in Astronomy and Astrophysics* **11** 924–946
[97] Andrae R, Fouesneau M, Creevey O, Ordenovic C, Mary N, Burlacu A, Chaoul L, Jean-Antoine-Piccolo A, Kordopatis G, Korn A, Lebreton Y, Panem C, Pichon B, Thévenin F, Walmsley G and Bailer-Jones C A L 2018 *A&A* **616** A8
[98] Ahumada R, Prieto C A, Almeida A, Anders F, Anderson S F, Andrews B H, Anguiano B, Arcodia R, Armengaud E, Aubert M, Avila S, Avila-Reese V, Badenes C, Balland C, Barger K, Barrera-Ballesteros J K, Basu S, Bautista J, Beaton R L, Beers T C and Benavides B I T 2020 *ApJS* **249** 3
[99] Guo Y, Zhang B, Liu C, Li J, Li J, Wang L, Liu Z, Hou Y H, Han Z and Chen X 2021 *ApJS* **257** 54
[100] Zhang B, Liu C and Deng L C 2020 *ApJS* **246** 9
[101] Gaia Collaboration, Brown A G A, Vallenari A, *et al.* 2021 *A&A* **649** A1
[102] Wang S and Chen X 2019 *ApJ* **877** 116
[103] Wang L, Li J, Wu Y, Gies D R, Liu J Z, Liu C, Guo Y, Chen X and Han Z 2022 *ApJS* **260** 35
[104] Guo Y, Li J, Xiong J, Li J, Wang L, Xiong H, Luo F, Hou Y, Liu C, Han Z and Chen X 2022 *Research in Astronomy and Astrophysics* **22** 025009
[105] Li J, Li J, Liu C, Li C, Guo Y, Wang L, Chen X, Xing L, Hou Y and Han Z 2022 *ApJ* **933** 119
[106] Astropy Collaboration, Price-Whelan A M, Sipőcz B M, *et al.* 2018 *AJ* **156** 123
[107] Taylor M B 2005 *Astronomical Data Analysis Software and Systems XIV* **347** 29